MADRID
inter.noise 2019
June 16 - 19
NOISE CONTROL FOR A BETTER ENVIRONMENT

Optimal actuator locations for flexible structures with free edges in active vibration control

Fu, Xiaohan
School of Marine Science and Technology, Northwestern Polytechnical University
No. 127, Youyi Road(West), Beilin, Xi'an City, Shaanxi Province, PRC
Sheng, Meiping[1]
School of Marine Science and Technology, Northwestern Polytechnical University
No. 127, Youyi Road(West), Beilin, Xi'an City, Shaanxi Province, PRC
Li, Qiaojiao
School of Marine Science and Technology, Northwestern Polytechnical University
No. 127, Youyi Road(West), Beilin, Xi'an City, Shaanxi Province, PRC
Han, Yuying
School of Marine Science and Technology, Northwestern Polytechnical University
No. 127, Youyi Road(West), Beilin, Xi'an City, Shaanxi Province, PRC

ABSTRACT

Locations of actuators greatly influence the effect of active vibration control, thus actuator placement is essential to the design of a control system. In this paper, optimized actuator locations for both beam and plate structures are discussed based on gramian controllability. Apparently various boundary conditions of a structure lead to different difficulties in obtaining the state space equation, especially for a two-dimensional plate. As a result, the flexible structures with free edges which space equations are more complex to obtain are studied. Further, both force actuators and piezoelectric actuators are discussed and the deduced equations show the space equations of which are totally different. Based above, the paper focuses on the optimal actuator locations for piezoelectric actuators and a detailed optimization process is displayed. Finally, the global response of feedforward active vibration control is displayed to validate the optimized result.

Keywords: Optimal location, Active vibration control, Structure with free edges
I-INCE Classification of Subject Number: 46

[1] smp@nwpu.edu.cn

1. INTRODUCTION

Active vibration control has been widely concerned by researchers for its excellent control effect in low-frequency domain. In the process of active vibration control, secondary sources are usually induced to counteract the original external exciting energy [1]. The secondary power is firstly calculated by control algorithms and then executed by actuators. To improve the vibration control effect, varies kinds of actuators have been designed. According to the characteristic of applied excitation, it can be divided into two modes, including point force excitation and moment excitation. The former is usually executed by shakers or exciters [2] while the later is performed by piezoelectric patches. At present, due to the high flexibility, durability and manufacturability [3], piezoelectric materials such as PVDF (Polyvinylidene fluoride) and MFC (Macro Fiber Composite) are highly applied in active vibration control.

Inappropriate placement of actuators will result in less effect or even invalid control. As a result, locations of actuators should be chosen carefully before active vibration control. To solve the problem, various optimization criteria have been proposed. Hac and Liu [4] proposed an open-loop optimized criteria for force actuators. A global energy index is adopted in the optimization procedure to maximize the controllability, and the simulation of simply supported structures are displayed. Based on this, Bruant [5] improved the criterion taking into account the residual modal component. Both force and piezoelectric active elements are considered separately for simply supported structures. Due to the wide applicability, many researchers have put forward optimized criteria based on the gramian controllability. According to the gramian controllability, it is necessary to acquire the state space equations. However, it is difficult to acquire the state equation for a flexible structure with free edges, for lack of analytical mode functions. Fujin Peng [6] proposed a method to obtain the electronic-mechanism coupling matrix using ANSYS. While a simulation for a cantilever plate is displayed, the control effect for limited locations are verified.

In this paper, the actuator location is optimized for structures under free boundary condition. Both force actuator and piezoelectric actuator are discussed separately. For piezoelectric actuator, an analytical method is proposed to construct the state equation for a plate with all 4 free edges. Further, the global attenuation effect is shown and compared with the effect at a randomly selected location to verify the proposed method.

2. MODELLING EQUATIONS

2.1 Point force actuators

Consider a structure controlled by several force actuators, finite element equation of which is represent as follows

$$M\ddot{V} + C\dot{V} + KV = F \tag{1}$$

The displacement of the structure can be expressed in modal coordinates

$$V = \Phi \eta \tag{2}$$

According to the modal orthogonality, the decoupled equation is obtained as

$$\ddot{\eta}_i + 2\xi\omega\dot{\eta}_i + \omega^2\eta_i = \sum_{j=1}^{P}\Phi_i{}^T(\mathrm{P}_j)\,f_i \tag{3}$$

where the subscript i denotes the ith vibration mode and the subscript j denotes the location of the jth force actuator. The coordinate transformation in the state space form is

$$x = [\dot{\eta}_i \;\; \ddot{\eta}_i] \tag{4}$$

The state space model is expressed as follows

$$\begin{bmatrix}\dot{\eta}_i \\ \ddot{\eta}_i\end{bmatrix} = \begin{bmatrix}0 & 1 \\ -\omega_i^2 & -2\xi_i\omega_i\end{bmatrix}\begin{bmatrix}\eta_i \\ \dot{\eta}_i\end{bmatrix} + \begin{bmatrix}0 & 0 & ..... & 0 \\ \Phi_i(\mathrm{P}_1) & \Phi_i(\mathrm{P}_2) & ..... & \Phi_i(\mathrm{P}_p)\end{bmatrix}\begin{bmatrix}f_1 \\ f_2 \\ \vdots \\ f_p\end{bmatrix} \tag{5}$$

Thus the control equation is

$$\dot{x} = Ax + Bu_a \tag{6}$$

where u_a is the output of actuators. In the case, the matrix u_a is a $p \times 1$ column vector for the output value of point forces.

2.2 Piezoelectric actuators

When a piezoelectric actuator (such as PVDF or MFC) is considered, the control equation becomes different. In the paper, an analytical method is presented as follows.

The forced vibration equation of a plate stimulated by a piezoelectric actuator is

$$D\nabla^4\xi + \rho h\ddot{\xi} = \frac{\partial^2 M_x}{\partial x^2} + \frac{\partial^2 M_y}{\partial y^2} \tag{7}$$

where $D = Eh^3/12(1-\mu^2)$ is the bending stiffness, M_x and M_y are the bending moments in x and y directions separately. According to reference [7], moment applied to the plate can be expressed as

$$M_x = M_{px}U_{ak}(t)[H(x-x_k) - H(x-x_{k-1})] \tag{8}$$

$$M_y = M_{py}U_{ak}(t)[H(y-y_k) - H(y-y_{k-1})] \tag{9}$$

Meanwhile, the displacement is described in the superposition form of two-dimension beam function

$$\xi(x,y,t) = \sum_{i=1}^{\infty}\sum_{j=1}^{\infty}\eta_{i,j}(x,y)T_{i,j}(t) = \sum_{i=1}^{\infty}\sum_{j=1}^{\infty}X_i(x)Y_j(y)T_{i,j}(t) \tag{10}$$

where $X_i(x)$ and $Y_j(y)$ are the vibration mode functions of a beam under the corresponding boundary situation. The subscripts i and j are the (i , j) mode along the x and y direction separately.

Substituting Equations 8-10 into Equation 7, the decoupled equation is obtained as

$$\frac{d^2T_{i,j}(t)}{dt^2}+2\xi_{i,j}\omega_{i,j}\frac{dT_{i,j}(\mathrm{t})}{dt}+\omega_{i,j}^2T_{i,j}(t)=\sum_{k=1}^{N_a}Q_{(i,j),k}(x,y)U_{ak}(t) \tag{11}$$

where Q is considered as the modal force of piezoelectric actuators

$$Q=\int_0^a\int_0^b\left(\frac{\partial^2M_x(x,y)}{\partial x^2}+\frac{\partial^2M_y(x,y)}{\partial y^2}\right)\eta(x,y)\,dydx \tag{12}$$

Substitute M_x and M_y into Equation 12, the modal force can be expressed as

$$Q_{i,j}=M_{ax}\left[X_i^{'}(x_2)-X_i^{'}(x_1)\right]\int_{y_1}^{y_2}Y_j(y)dy+M_{ay}\left[Y_j^{'}(y_2)-Y_j^{'}(y_1)\right]\int_{x_1}^{x_2}X_i(x)dx \tag{13}$$

For a rectangular plate with 4 free edges, both X and Y are the modal functions of free-free beam. However, the common combination of trigonometric function cannot meet the boundary conditions. As a result, the improved Fourier series expansions [8] are used to express its displacement as follows

$$X(\mathrm{x})=\sum_{m=0}^{\infty}A_m\cos\frac{m\pi x}{a}+c^1\sin(\frac{\pi x}{2a})+c^2\cos(\frac{\pi x}{2a})+c^3\sin(\frac{3\pi x}{2a})+c^4\cos(\frac{3\pi x}{2a}) \tag{14}$$

Here the state space equation is directly displayed as follows

$$\dot{x}=Ax+Bu \tag{15}$$

in which, $x=\left(\omega_{i,j}T_{i,j}\quad \dot{T}_{i,j}\right)^T$, $\mathbf{a}=\begin{pmatrix}0 & \omega_{i,j}\\ -\omega_{i,j} & -2\xi_{i,j}\omega_{i,j}\end{pmatrix}$, $i=1,2,...,m_x$, $j=1,2,...,m_y$,

$\mathrm{A}=diag\{\mathbf{a}\}$, $B=\begin{bmatrix}0 & Q_{1,1} & 0 & Q_{1,2} & \cdots & 0 & Q_{i_1,j_1}\end{bmatrix}^T$, $i_1=1,2,...,M$, $j_1=1,2,...,\mathrm{N}$.

3. CONTROLLING EQUATIONS

When a single piezoelectric actuator is considered, the optimal control voltage is calculated according to the feedforward algorithm [14]. Assuming that the displacement response of an error sensor can be regarded as a linear superposition of the response caused by various loads, it can be expressed as

$$W_e=W_p+W_s=V_pG_{pe}+V_sG_{se} \tag{16}$$

where W_p and W_s are the displacements induced by the single primary actuator and the secondary actuator separately. And W_e is the displacement of error sensor that can be measured directly in the experiment. G_{pe} and G_{se} are the displacement responses of error sensor when a unit voltage are applied to the primary actuator and secondary actuator individually.

While the squared displacement of the error sensor is regarded as the objective function, the optimal control voltage can be calculated as

$$V_{s,opt}=-V_p\frac{B_{ps}}{A_{ss}} \tag{17}$$

where $A_{ss} = G_{se} \cdot G_{se}^{*}$, $B_{ps} = G_{pe} \cdot G_{se}^{*}$.

4. OPTIMIZATION CRITERIA FOR ACTUATOR LOCATIONS

In terms of searching the optimized location of actuators, myriad methods have been proposed. The main idea of those optimized methods is to set up a cost function. In this paper, the commonly used gramian controllability is adopted. The controllability gramian matrix is expressed as

$$W(\mathrm{T}) = \int_0^T e^{At} B B^T e^{A^T t} dt \tag{18}$$

Any small eigenvalue of the gramian matrix will lead to control failure of the relevant mode [9]. From Equation 15, it is clear that the input matrix *B* which includes the position information is related to the gramian matrix. When the structural damping is small, through the solution of a Lyapunov equation, the gramian matrix can be transformed to a diagonal form [4]

$$w_c = diag\{w_{c1}, w_{c2}, ..., w_{cn}\} \tag{19}$$

where w_{ci} is the ith eigenvalue of the gramian matrix.

The proposed criteria in reference [10] is adopted for the following simulation, which is shown as

$$\max\{\min_{i=1,...,N} w_{co}(\mathrm{A}_1, \mathrm{A}_2, ..., \mathrm{A}_{Na}) - \lambda \min_{i=1,...,N^R} w_{unco}(\mathrm{A}_1, \mathrm{A}_2, ..., \mathrm{A}_{Na})\} \tag{20}$$

where $w_{co} = \left(\sum_{i=1}^{N_c} w_{ci}\right) \sqrt[N_c]{\prod_{i=1}^{N_c} w_{ci}} \Big/ \sigma(w_{ci})$, $w_{unco} = \left(\sum_{i=1}^{N_u} w_{ui}\right) \sqrt[N_u]{\prod_{i=1}^{N_u} w_{ui}} \Big/ \sigma(w_{ui})$.

The summation above represents the transferred energy from actuators to the controlled structure while the product item represents the average change rate of control energy. Besides, the standard deviation is adopted to avoid extremely large or small datasets.

4. SIMULATION EXAMPLES

In this section, a detailed optimization process for a plate under free boundary condition is displayed. The geometry parameters of the plate are 1.8m×1.0m with thickness of 3mm. The optimized location of piezoelectric actuator is considered to acquire a good control effect for the first 6 modes. The first 6 mode shapes of the free-boundary rectangular plate are shown in Figure 1.

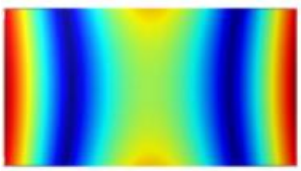

1st, 4.9Hz

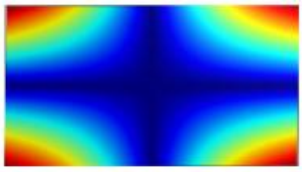

2nd, 5.6Hz

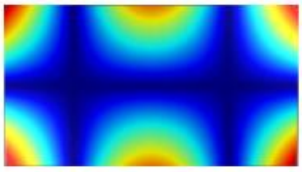

3rd, 12.4Hz

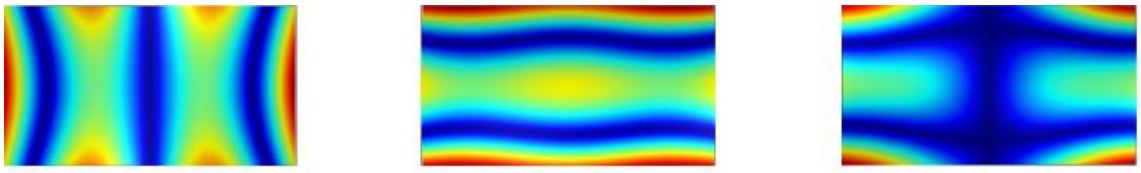

Figure 1: Mode shape of the plate with free edges

The flexible plate is divided into 180×100 blocks and each block is regarded as a candidate location for piezoelectric actuator. Assuming that 100 voltage is separately applied to each actuator, the matrix Q can be obtained through Equation 8-10 and Equation 13-14. Thus the matrix B (Equation 14) is obtained for the gramian matrix. According to Equation 17, the criterion index for candidate placements are calculated and the optimization result is shown in Figure 2. When only one actuator is considered, the optimal location is at (0.58m, 0.31m). Placement of multi-channel actuators can also be decided by Equation 15, with the method of genetic algorithms [11-12]. In the next section, the optimized result will be verified for the case of single actuator.

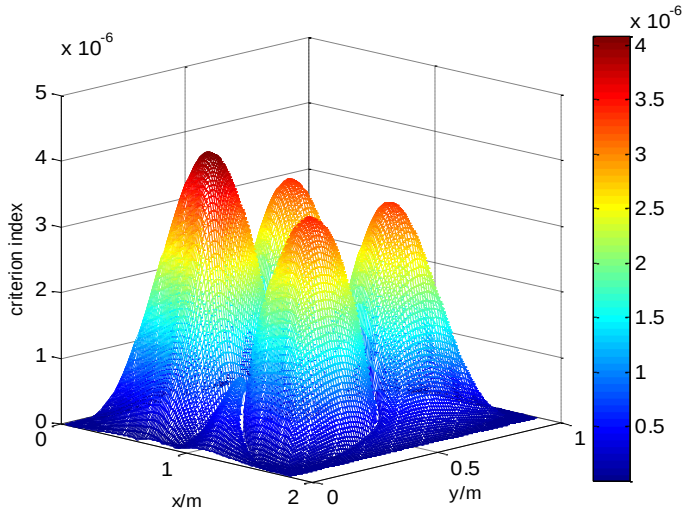

Figure 2: Optimization result for the plate with free edges

5. SIMULATION VERIFICATION AND DISCUSSION

In this section, the optimized result for the location of piezoelectric actuator is discussed. The location of (0.24m, 0.2m) is chosen randomly for comparison. To verify the feasibility of the optimized location, the feedforward active control is applied and the simulation geometry is shown in Figure 3.

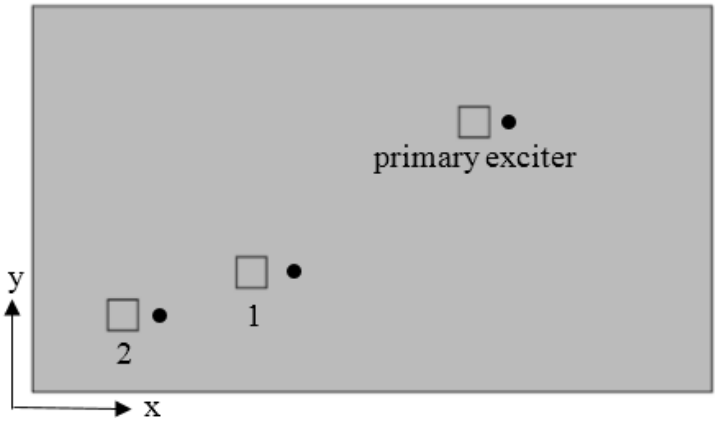

Figure 3: Location of Actuators

As shown in Figure 3, the actuator labeled 1 refers to the optimized location and the actuator labeled 2 refers to the comparative location. Every error sensor (solid dot) is collocated with the actuator so as to guarantee the stability of the control system [13]. Besides, the third one is regarded as the primary exciter, which ensures that all the required modes are well excited. In the subsequent simulation, PVDF patches are selected for actuators, which material parameters are listed in Table 1.

Table 1: PVDF Material Parameters

	Parameters
Density (kg/m^3)	1780
Young's modulus (MPa)	2500
Poisson's ratio	0.35
D_{31}, D_{32}, D_{33} (Pc/N)	17, 5, -21
Relative permittivity	9500

During the active control process, the voltage of 100V is applied to actuator 1 as external disturbance. Equation 17 is implemented to calculate the optimal control voltage. The active control effects of the first 6 structural vibration modes are individually shown in Figure 4. To illustrate the control effect of the two compared locations, the counter range (the right) has been unified dividedly for every frequency according to the control effect of optimized position (the left). A color scale is showed below to indicate the relative magnitude of displacement response.

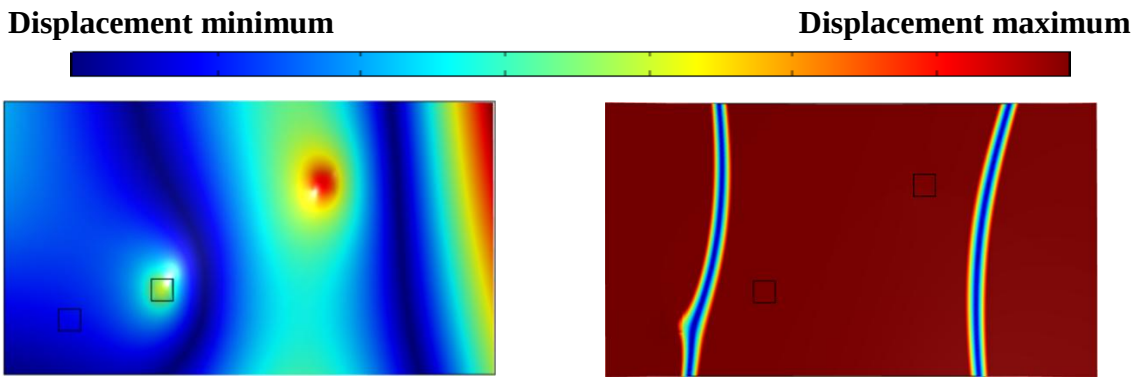

(a) Control effect of the 1st mode

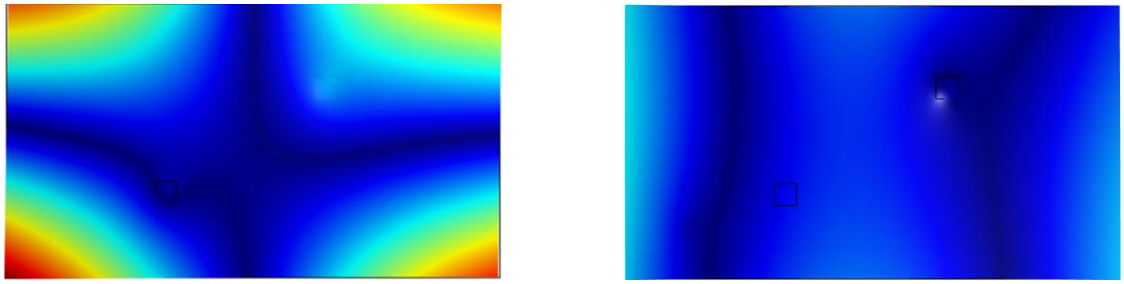

(b) Control effect of the 2nd mode

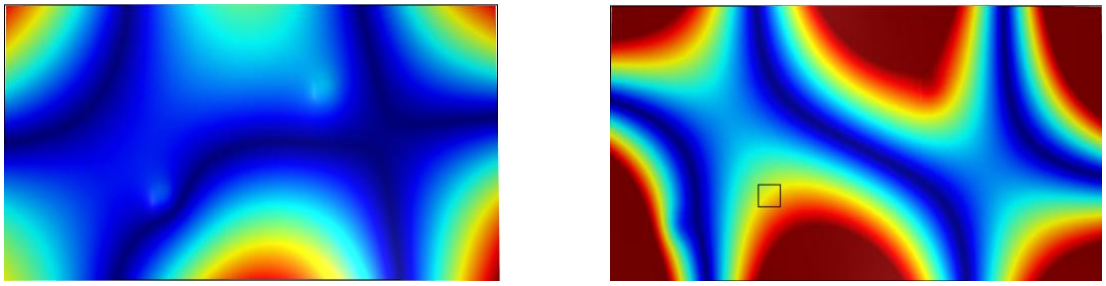

(c) Control effect of the 3rd mode

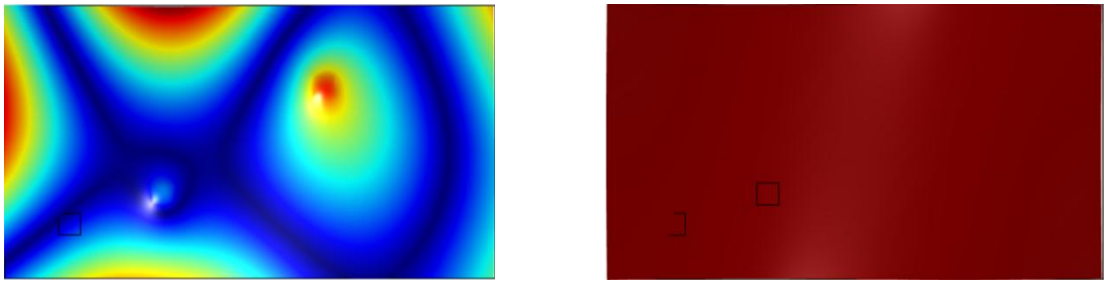

(d) Control effect of the 4th mode

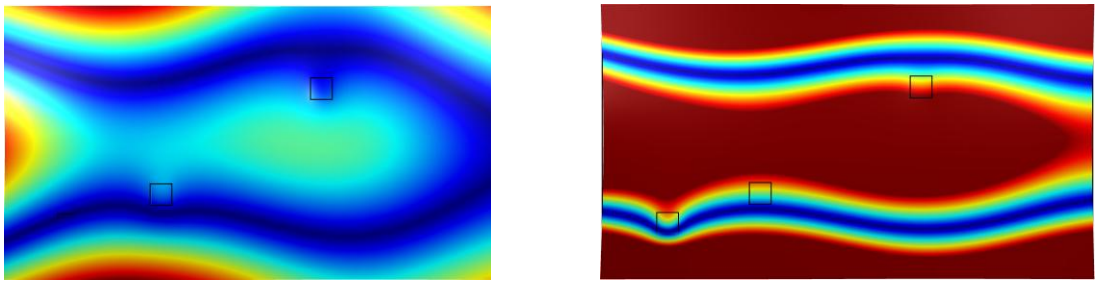

(e) Control effect of the 5th mode

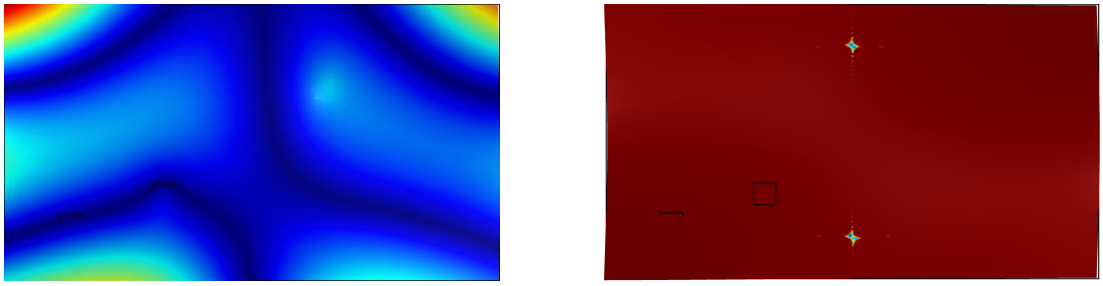

(f) Control effect of the 6th mode

Figure 4: Active control effect (left: optimized location; right: compared location)

As shown in Figure 4, the actuator located at the optimized location has a better control effect within the concerned frequency range. Meanwhile, the actuator at the compared location fell to control for some frequency, which is not expected to happen in practical engineering. It should be noted that although slightly better control effect is achieved at the second mode by compared actuator, the optimized actuator still gains a global attenuation compared with the uncontrolled structural response.

Further, to give a direct comparison of the required output energy, the calculated optimal control voltages of actuator 1 and actuator 2 are listed in Table 2.

Table 2: Control voltage in feedforward active control (Primary excitation voltage: 100V)

Controlled Mode	Optimal Location	Compared Location
1	-109.37 V	-441.78 V
2	-100.06 V	-47.97 V
3	126.36 V	-191.02 V
4	93.29 V	-191.98 V
5	-103.55 V	-550.42 V
6	88.45 V	-271.8 V

It can be seen that less energy is required for the optimized actuator, except for the second mode. While the optimal control voltage is within the acceptable range for the second mode, more energy is needed for the compared actuator. Thus the optimized result for a plate with 4 free edges is verified from the aspect of global control effect and energy requirement respectively.

6. CONCLUSION

In this paper, optimal actuator location for a rectangular flexible plate with 4 free edges is studied analytically and both force actuator and piezoelectric actuator are considered. For piezoelectric actuator, the two-dimension beam function method is adopted to obtain the state space equations, and optimal location for a secondary actuator is calculated

according to gramian controllability. The optimized result is verified through feedforward active control method and the global control effect is displayed. In contrast with the compared location, the optimized actuator can achieve an effective global attenuation for low frequency modes and requires less energy for the control system.

7. REFERENCES

1. Burdisso R A , Fuller C R , Suarez L E . *Adaptive Feedforward Control of Structures Subjected to Seismic Excitation*, American Control Conference. IEEE, (1993).
2. Keir J , Kessissoglou N J , Norwood C J . *Active control of connected plates using single and multiple actuators and error sensors*, Journal of Sound and Vibration, 281(1-2):73-97, (2005).
3. Tzou H S , Tseng C I . *Distributed piezoelectric sensor/actuator design for dynamic measurement/control of distributed parameter systems: A piezoelectric finite element approach*. Journal of Sound and Vibration, 138(1):17-34, (1990).
4. Hać A. *Sensor And Actuator Location In Motion Control of Flexible Structures*. Journal of Sound & Vibration, 167(2):239–261, (1993).
5. Bruant I, Proslier L. *Optimal location of piezoelectric actuators for active vibration control of thin axially functionally graded beams*. Journal of Sound & Vibration, 329(10):1615-1635, (2010).
6. Peng, F. *Actuator Placement Optimization and Adaptive Vibration Control of Plate Smart Structures*. Journal of Intelligent Material Systems and Structures, 16(3):263-271, (2005).
7. Abreu G. L. C. M. D, Ribeiro J F, Steffen V. *Finite element modeling of a plate with localized piezoelectric sensors and actuators*. Journal of the Brazilian Society of Mechanical Sciences and Engineering, 26(2):117-128, (2004).
8. Zhang A F, Sheng M P, Zhao Z M, et al. *Power flow analysis of a multi-span coupled plate using Fourier series expansion*. Journal of Vibration & Shock, 32(14):103-108, (2013).
9. ARBEL, AMI. *Controllability measures and actuator placement in oscillatory systems*. International Journal of Control, 33(3):565-574, (1981).
10. Leleu S , Abou-Kandil H. Bonnassieux Y . *Piezoelectric actuators and sensors location for active control of flexible structures*. IEEE Transactions on Instrumentation and Measurement, 50(6):1577-1582, (2001).
11. Han J H , Lee I. *Optimal placement of piezoelectric sensors and actuators for vibration control of a composite plate using genetic algorithms*. Smart Materials and Structures, 8(2):257-267, (1999).
12. Biglar M, Gromada M, Stachowicz F, et al. *Optimal configuration of piezoelectric sensors and actuators for active vibration control of a plate using a genetic algorithm*. Acta Mechanica, 226(10):3451-3462, (2015).
13. Lee Y S. *Comparison of collocation strategies of sensor and actuator for vibration control*. Journal of Mechanical Science and Technology, 25(1):61-68, (2011).
14. Brennan M J, Elliott S J, Pinnington R J. *Strategies for the active control of flexural vibration on a beam*. Journal of Sound and Vibration, 186(4):657-688, (1995).